Progress In Electromagnetics Research M, Vol. 110, 157–169, 2022

On the Performance of Reconfigurable Intelligent Surface in Cooperative Decode-and-Forward Relaying for Hybrid RF/FSO Systems

Kehinde O. Odeyemi[1, *], Pius A. Owolawi[2], and Oladayo O. Olakanmi[1]

Abstract—Reconfigurable intelligent surface (RIS) has been suggested as a promising solution to prevent wireless communication systems from transmission blockage. In this paper, the performance of reconfigurable intelligent surface in cooperative decode-and-forward relaying for hybrid radio frequency (RF)/free space optical (FSO) system is evaluated where parallel transmission of information occurs on the system downlink. In this network, the RF links in the system are assumed to follow Nakagami-m distributions while the FSO link is subjected to Gamma-Gamma distribution. Thus, the exact closed-form expressions of the system outage probability and average bit error rate are obtained to quantify the system performance. The accuracy of these expressions is justified by Monte-Carlo simulations. Also, to get more physical insight from the derived outage probability expression, the asymptotic outage probability under the condition of higher signal-to-noise ratio (SNR) is provided. In addition, the results illustrate that the system and channel parameters significantly affect the performance of the concerned system. Furthermore, the results show that RIS-hybrid downlink system offers better performance than hybrid downlink system without RIS. Under the RIS system, the results demonstrate that RIS-hybrid downlink system outperforms RIS-FSO downlink system.

1. INTRODUCTION

Reconfigurable intelligent surface (RIS) has gained tremendous interest in the research community due to its capability to prevent transmission blockage by controlling the direction in which radio waves are reflected between the source and the final destination [1, 2]. Also, it enhances the focus of the radio waves beam in order to extend the coverage area of the system transmission. As an emerging technology, it is artificial planar surface made of electromagnetic (EM) materials which can effectively control the characteristics of incident signal such as phase, amplitude, and frequency [3, 4]. Compared to the conventional relaying and multiantenna technologies, it requires no RF chain and additional power for signal amplification, transmission, and regeneration [5]. Therefore, they are more economical and environmental friendly compared to active antenna systems counterpart [6]. With these great features, it is very easy to integrate RISs into existing wireless network by deploying them on structures such as building surfaces, windows, human cloths, and roadside billboards [7]. Based on these advantages of RIS, a lot of research studies have exploited RIS to enhance the performance of existing wireless communication systems. In [8], RIS was employed to enhance the performance of high altitude platform for multiusers communication. Also, RIS was used in [5] to improve the coverage area of unmanned aerial vehicle (UAV) communication system where the outage probability and system error rate were evaluated. Moreover, the performance analysis of a multilayer UAV wireless communication with the assistance of

Received 6 February 2022, Accepted 7 May 2022, Scheduled 24 May 2022
* Corresponding author: Kehinde Oluwasesan Odeyemi (kesonics@yahoo.com).
[1] Department of Electrical and Electronic Engineering, Faculty of Technology, University of Ibadan, Nigeria. [2] Department of Computer Systems Engineering, Tshwane University of Technology, Pretoria 0001, South Africa.

RIS was studied in [9]. The authors in [10] proposed an RIS-aided power line communication system under different system relay protocols.

Recently, hybrid RF/FSO communication has been suggested as a powerful candidate for wireless backhaul networks. With the advantages of FSO link such as high date rate, unlicensed and unregulated optical spectrum, easy deployment, etc., the link suffers from various channel impairments in its practical implementation. In this case, FSO link is highly prone to atmospheric turbulence due to inhomogeneities in the atmospheric pressure and temperature as a result of variation in refractive index leading to rapid fluctuation in optical signal [11]. As a light-of-sight (LOS) link, it is usually affected by pointing errors due to misalignment between the transmitter and the receiver as a result of building sway [12]. Mainly, the FSO link suffers from attenuation due to fog but is less sensitive to rain conditions. RF communication link on the other hand is a reliable link in fog weather conditions [13]. However, the link is subjected to multipath fading and highly susceptible to heavy rain conditions. It has also reached a bottleneck due to spectrum scarcity [14]. Therefore, the complementary features of RF and FSO links have led to the implementation of hybrid RF/FSO system. Different approaches have been proposed in literature to guarantee reliable transmission in hybrid RF/FSO systems. The first approach is parallel transmission in which identical information is transmitted on both RF and FSO links. However, this approach wastes power and causes unnecessary interference [15]. The second approach is hard switching where the channel state information is used to select transmission link between the RF and FSO links. This approach requires a feedback from the destination to source and offers the system efficient transmission at high date rate [16]. The third approach is soft switching which is the most complex approach, employs joint coding for both RF and FSO links under channel conditions [17].

Cooperative relaying technology is one of the promising techniques to improve the reliability and coverage area of the wireless systems. The concept involves the transmission of source information to the destination via relay node(s). The relaying strategies can be classified as amplified-and-forward (AF) and decode-and-forward (DF) relaying protocol. In AF relaying protocol, the relay node amplifies the source information and forwards the amplified copy to the destination. On the other hand, DF relaying protocol involves the relay node decoding the source information before it is transmitted to the destination [2]. It is confirmed that hybrid RF/FSO systems establish short range transmission. Consequently, to extend the system coverage area, dual-hop cooperative relaying hybrid RF/FSO systems have been thoroughly studied in open literature where RF and FSO links are used in both hops. In [14], a switching based cooperative DF relaying for a hybrid RF/FSO system with direct FSO link was presented. Also, the authors in [18] compared the performance of a single-hop hybrid RF/FSO satellite system with a dual-hop hybrid RF/FSO satellite system. Under the dual-hop system, the FSO line was considered for the first hop while the hybrid RF/FSO link was used in the second hop. The results illustrated that the dual-hop hybrid system was able to perform better than single-hop hybrid system. Moreover, the performance of a relay selection in dual-hop hybrid RF/FSO satellite network was investigated in [19]. In this study, the system employing FSO links between the satellite and the relays in the first hop and hybrid RF/FSO transmission was established between the relays and the ground stations in the second hop. Ninos et al. in [20] studied the performance of a dual-hop full-duplex DF relaying system where each hop consists of a parallel hybrid RF/FSO link. In addition, the performance analysis of DF multi-hop hybrid RF/FSO system under the hard switching scheme was presented in [21], where the outage probability and ergodic capacity of the system were obtained under the effect of different weather conditions. The outage probability of an AF dual-hop based hybrid RF/FSO system under different relaying methods was presented in [22]. In all these stated works on the dual-hop hybrid RF/FSO systems, however, reconfigurable intelligent surface was not considered for signal transmission. In the context of RIS as cooperative relay, the authors in [23] employed RIS to enhance the performance of a mixed dual-hop FSO/RF communication system under the influence of hybrid automatic repeat request protocol. Also, performance of a dual-hop FSO/RF communication link was studied in [24] where RIS was used to aid the performance of each hop. Moreover, a multi-hop RIS-assisted FSO/RF system for vehicular communication was studied in [1] where multiple RISs were adopted between the RF and FSO links for multi-hop transmission. In addition, mixing RIS-equipped RF sources with FSO links were studied in [25] where the RF sources were deployed with multiple RISs and adopted opportunistic scheduling for signal transmission. The effect of co-channel interference (CCI) on the RIS-assisted mixed

FSO/RF system was investigated in [26] with the destination corrupted by CCI. Malik et al. [27] studied the performance of a UAV-based RIS-assisted FSO/RF system under the effects of pointing errors and phase error. However, in all these aforementioned research works on the dual-hop RIS-assisted RF/FSO systems, information signal was not simultaneously transmitted on both RF and FSO links at the same time but was transmitted in hops between the RF and FSO links. Therefore, the link between the RIS and destination (downlink) of the pervious works was based on a single link that is either RF or FSO link. Thus, the necessary comparison between our proposed system and previous works on hybrid RF/FSO system is provided in Table 1.

Table 1. Comparison of proposed system with previous works.

Reference	RIS technique	Single transmission at downlink	Parallel transmission at downlink
[14]	×	×	√
[18]	×	×	√
[19]	×	×	√
[20]	×	×	√
[21]	×	×	√
[22]	×	×	√
[1]	√	√	×
[23]	√	√	×
[24]	√	√	×
[25]	√	√	×
[26]	√	√	×
[27]	√	√	×
Proposed Work	√	√	√

Motivated by above observations, the reconfigurable intelligent surface in cooperative DF relaying for hybrid RF/FSO system is investigated in this paper where the downlink transmission of information occurs simultaneously of both RF and FSO after reflection of signal from RIS. Thus, the closed-form expressions for the system outage probability and average bit error rate (BER) are derived. Also, the asymptotic expression of the outage probability is obtained at high SNR regime to provide more physical insight into the performance of the concerned system. It is worthwhile to state here that central limit theorem was considered in the analysis of most of the previous works on RIS-assisted systems, and this amount to a large number of reflecting elements. Following other approaches, Nakagami-m fading channel for limited number of reflecting elements is considered in the analysis of this concerned system. The specific contributions of this work are summarized as follows:

i. The analytical closed-form analytical expressions of the outage probability and average BER are derived and serve as key metrics to evaluate the performance of the concerned system.
ii. Moreover, the asymptotic outage probability of the system is obtained at high SNR in order to get more physical insight about the system performance.
iii. Relative to dual-hop hybrid RF/FSO systems in [14, 18–20, 22], the proposed system presented in this paper is RIS-assisted dual-hop hybrid RF/FSO.
iv. Relative to RIS-mixed RF/FSO system in [1, 23, 24], the downlink of the proposed system involves parallel transmission of information on both RF and FSO links.

The remainder of this paper is structured as follows. Section 2 demonstrates the system and channel models. The performance analysis of the system with asymptotic analysis is detailed in Section 3. In Section 4, the numerical results with discussions are presented. Finally, Section 5 gives the paper conclusion remarks.

2. SYSTEM AND CHANNEL MODELS

An RIS assisted hybrid RF/FSO system is illustrated in Figure 1 where hybrid RF/FSO relay node assists the source (S) to send its message to destination via an RIS with N_E reflecting elements. It is assumed that the relay node adopts DF relaying protocol to transmit source information from RIS to the destination via the parallel RF and FSO links. Due to higher data rate, FSO link is set to have higher priority. The RF links within the network are subjected to Nakagami-m distributions while the FSO link follows Gamma-Gamma distributions. It is also assumed that there is transmission blockage between the source and the destination due to obstacles such as hills, buildings, and aeroplane. The concerned system utilizes two-phase orthogonal transmissions.

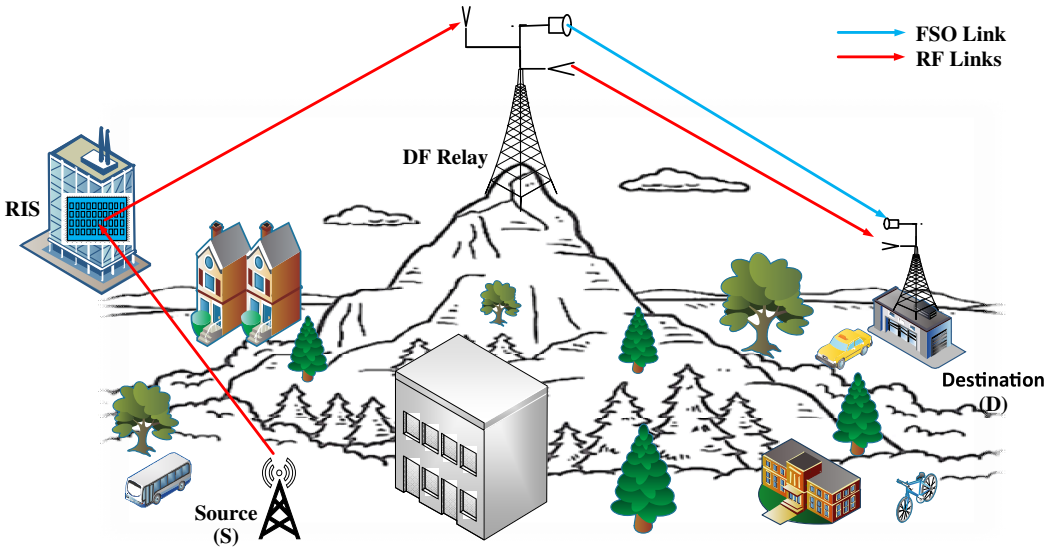

Figure 1. RIS-assisted hybrid RF/FSO system model.

During the first phase, the source sends its signal to the RIS which is reflected with optimal phase to the relay node. During the second phase, the relay transmits the source decoded signal over the hybrid RF/FSO communication link. At the destination, the selection combiner is used to select the maximum signal-to-noise (SNR) between the two links. If the FSO instantaneous SNR is above a predefined threshold, the FSO link will be used by source for signal transmission. Otherwise, a 1-bit feedback signalling is sent to activate the RF sub-link, and the source signal will be transmitted over RF link. Thus, the instantaneous SNR of the RF link can be given $\gamma_i = \bar{\gamma}_i |h_i|^2$ where $i \in \{1, 2\}$ and $\bar{\gamma}_i$ is the average SNR of the RF link with the h_i being the channel gain of the link. The channel gain of the RIS link is defined as $h_1 = \sum_{n=1}^{N} g_n \upsilon_n$ with g_n and υ_n being independently Nakagami-m distributed random variables with shape parameter m. In addition, the instantaneous SNR of the FSO link can be given as $\gamma_3 = \bar{\gamma}_3 |I|^2$ with the $\bar{\gamma}_3$ denoting the average SNR of the FSO link, and I signifies the link channel gain.

It is assumed that the source-RIS-relay links undergo Nakagami-m distribution, and the probability distribution function (PDF) of the instantaneous SNR of the link can be expressed as [28]:

$$f_{RIS}(\gamma) \approx \frac{\exp\left(-\gamma^{1/2}/\sqrt{\bar{\gamma}_1 \mu_2^2}\right)}{2\mu_2^{\mu_1+1}\Gamma(\mu_1+1)\,\bar{\gamma}_1^{(\mu_1+1)/2}}\,\gamma^{\frac{\mu_1-1}{2}} \tag{1}$$

where

$$\begin{cases} \mu_1 = \dfrac{(N_E+1)\,\Gamma(m_i+1/2)^4 - m_i^2\Gamma(m_i)^4}{m_i^2\Gamma(m_i)^4 - \Gamma(m_i+1/2)^4} \\ \mu_2 = \dfrac{m_i\Omega\left(\Gamma(m_i)^2\,\Gamma(m_i+1)^2 - \Gamma(m_i+1/2)^4\right)}{\Gamma(m_i+1/2)^2\,\Gamma(m_i+1)^2} \end{cases} \tag{2}$$

N_E represents the number of RIS elements, and m_i is the fading parameter of RIS link.

By integrating the link PDF given in (1) through the identity detailed in [29, Eq. (3.351(1))], the cumulative distribution function (CDF) of the link can be obtained as:

$$F_{RIS}(\gamma) \approx \frac{1}{\Gamma(\mu_1+1)}\,\gamma\left(\mu_1+1,\ \frac{\gamma^{\frac{1}{2}}}{\sqrt{\bar{\gamma}_1\mu_2^2}}\right) \tag{3}$$

where $\gamma(.,.)$ is the incomplete Gamma function.

Moreover, the link CDF can also be obtained in terms of Meijer-G function by converting the incomplete Gamma function in (3) to Meijer-G function using the identity detailed in [30, Eq. (8.4.16(1))] as:

$$F_{RIS}(\gamma) \approx \frac{1}{\Gamma(\mu_1+1)}\,G_{1,2}^{1,1}\left(\frac{\gamma^{\frac{1}{2}}}{\sqrt{\bar{\gamma}_1\mu_2^2}}\,\middle|\,\begin{matrix}1\\ \mu_1+1,\,0\end{matrix}\right) \tag{4}$$

Also, the RF sub-link between the relay and the destination is assumed to follow Nakagami-m distribution, and the PDF of the ink instantaneous SNR can be defined as [31]:

$$f_{RF}(\gamma) = \frac{\gamma^{m_f-1}}{\Gamma(m_f)\,\lambda^{m_f}}\,\exp(-\gamma/\lambda) \tag{5}$$

where $\lambda = \bar{\gamma}_2/m_f$ with m_f denoting the link fading parameter.

The CDF of the link can be obtained by integrating (5) using the integral identity defined in [29, Eq. (3.351(1))] as:

$$F_{RF}(\gamma) = \frac{1}{\Gamma(m_f)}\,G_{1,2}^{1,1}\left(\frac{\gamma}{\lambda}\,\middle|\,\begin{matrix}1\\ m_f,\,0\end{matrix}\right) \tag{6}$$

The FSO sub-link between the relay and the destination is assumed to experience Gamma-Gamma distribution. The PDF of the link by considering heterodyne detection at the destination can be expressed as [32]:

$$f_{FSO}(\gamma) = \vartheta\gamma^{-1}\,G_{1,3}^{3,0}\left(\frac{\Omega\gamma}{\bar{\gamma}_3}\,\middle|\,\begin{matrix}\xi^2+1\\ \xi^2,\alpha,\beta\end{matrix}\right) \tag{7}$$

where $\vartheta = \xi^2/\Gamma(\alpha)\Gamma(\beta)$ and $\Omega = \xi^2\alpha\beta/(1+\xi^2)$ with $\Gamma(\cdot)$ signifying the Gamma function; ξ signifies the pointing error; α and β are the scintillation parameters which are specified in [33]. Also, the link CDF can be expressed as:

$$F_{FSO}(\gamma) = \vartheta G_{2,4}^{3,1}\left(\frac{\Omega\gamma}{\bar{\gamma}_3}\,\middle|\,\begin{matrix}\xi^2+1,\,1\\ \xi^2,\alpha,\beta,0\end{matrix}\right) \tag{8}$$

3. PERFORMANCE ANALYSIS

In this section, outage probability and average bit error rate (ABER) are the two-performance metrics considered to quantify the performance of the concerned system.

3.1. Outage Performance

This describes the probability that the instantaneous SNR of the RIS and hybrid RF/FSO link falls below predefined SNR γ_{th}. The outage probability for the concerned system can be expressed as [34]:

$$P_{out}(\gamma_{th}) = Pr(\min(\gamma_{SR},\gamma_{RD}) < \gamma) \tag{9}$$

This can be further expressed as:

$$P_{out}(\gamma_{th}) = F_{SR}(\gamma) + (1 - F_{SR}(\gamma))\,F_{RD}(\gamma) \tag{10}$$

where $F_{SR}(\gamma)$ and $F_{RD}(\gamma)$ are the CDF of the source to relay link and relay-to-destination link, respectively. The relay-to-destination link can be defined as:

$$F_{RD}(\gamma) = F_{RF}(\gamma)\,F_{FSO}(\gamma) \tag{11}$$

By invoking (6) and (8) into (11), $F_{RD}(\gamma)$ can be obtained as:

$$F_{RD}\left(\gamma\right)=\frac{F_{SR}\left(\gamma\right)}{\Gamma\left(m_f\right)}G_{1,2}^{1,1}\left(\frac{\gamma}{\lambda}\middle|\begin{array}{c}1\\ m_f,\,0\end{array}\right)G_{2,4}^{3,1}\left(\frac{\Omega\gamma}{\bar{\gamma}_3}\middle|\begin{array}{c}\xi^2+1,\,1\\ \xi^2,\alpha,\beta,0\end{array}\right) \tag{12}$$

Substituting (11) and (12) into (10), then the system outage probability can thus be expressed as:

$$\begin{aligned}P_{out}\left(\gamma_{th}\right)\;=\;1-&\left(1-\frac{1}{\Gamma\left(\mu_1+1\right)}G_{1,2}^{1,1}\left(\frac{\gamma_{th}^{\frac{1}{2}}}{\sqrt{\bar{\gamma}_1\mu_2^2}}\middle|\begin{array}{c}1\\ \mu_1+1,\,0\end{array}\right)\right)\\&\left(1-\frac{\vartheta}{\Gamma\left(m_f\right)}G_{1,2}^{1,1}\left(\frac{\gamma}{\lambda}\middle|\begin{array}{c}1\\ m_f,\,0\end{array}\right)G_{2,4}^{3,1}\left(\frac{\Omega\gamma_{th}}{\bar{\gamma}_3}\middle|\begin{array}{c}\xi^2+1,\,1\\ \xi^2,\alpha,\beta,0\end{array}\right)\right)\end{aligned} \tag{13}$$

3.1.1. Asymptotic Outage Probability

Due to the complexity of the outage probability given in (13), limit information about the concerned system is obtained. Thus, asymptotic outage probability of the system at high SNR can be obtained as [35]:

$$F_{out}^{\infty}\left(\gamma_{th}\right)\approx F_{SR}^{\infty}\left(\gamma\right)+F_{RD}^{\infty}\left(\gamma\right) \tag{14}$$

where $F_{SR}^{\infty}(\gamma)=F_{RIS}^{\infty}(\gamma)$ and $F_{RD}^{\infty}(\gamma)=F_{RF}^{\infty}(\gamma)F_{FSO}^{\infty}(\gamma)$.

By utilizing the identity detailed in [29, Eq. (8.354(1))], the asymptotic expression for the $F_{RIS}^{\infty}(\gamma)$ can be obtained as:

$$F_{RIS}^{\infty}\left(\gamma\right)=\frac{1}{\Gamma\left(\mu_1+1\right)}\sum_{j=0}^{\infty}\frac{\left(-1\right)^j\left(\sqrt{\frac{\gamma}{\bar{\gamma}_1\mu_2^2}}\right)^{\mu_1+1+j}}{j!\left(\mu_1+1+j\right)} \tag{15}$$

By considering the first term of (15) as $\bar{\gamma}_1\to\infty$, the asymptotic expression for $F_{RIS}^{\infty}(\gamma)$ can be further expressed as:

$$F_{RIS}^{\infty}\left(\gamma\right)=\frac{\gamma^{(\mu_1+1)/2}}{\Gamma\left(\mu_1+1\right)\left(\mu_1+1\right)\left(\bar{\gamma}_1\mu_2^2\right)^{(\mu_1+1)/2}} \tag{16}$$

By obtaining the asymptotic series expansion of Meijer-G function through the identity detailed in [6, 29], the asymptotic expression for the $F_{RF}^{\infty}(\gamma)$ as $\bar{\gamma}_2\to\infty$ can be expressed as:

$$F_{RF}^{\infty}\left(\gamma\right)=\frac{1}{\Gamma\left(m_f+1\right)}\left(\frac{\gamma}{\lambda}\right)^{m_f} \tag{17}$$

Using a similar approach to that in the case of (17), the asymptotic expression for the $F_{FSO}^{\infty}(\gamma)$ as $\bar{\gamma}_3\to\infty$ can be expressed as:

$$F_{FSO}^{\infty}\left(\gamma\right)=\sum_{l=1}^{3}\frac{\prod_{\substack{t=1\\ l\neq t}}^{3}\Gamma\left(b_t-b_l\right)\Gamma\left(1-a_1+b_t\right)}{\Gamma\left(a_2-b_l\right)\Gamma\left(1-b_4+b_l\right)}\left(\frac{\Omega\gamma}{\bar{\gamma}_3}\right)^{b_l} \tag{18}$$

At high SNRs, the asymptotic outage probability of the system can be obtained by substituting (16), (17), and (18) into (14) as follows:

$$F_{out}^{\infty}\left(\gamma_{th}\right)\approx\frac{\gamma^{\frac{(\mu_1+1)}{2}}}{\Gamma\left(\mu_1+1\right)\left(\mu_1+1\right)\left(\bar{\gamma}_1\mu_2^2\right)^{\frac{(\mu_1+1)}{2}}}+\frac{1}{\Gamma\left(m_f+1\right)}\sum_{l=1}^{3}\delta_{fso}\left(\frac{\Omega\gamma}{\bar{\gamma}_3}\right)^{b_l}\left(\frac{\gamma}{\lambda}\right)^{m_f} \tag{19}$$

where

$$\delta_{fso}=\frac{\prod_{\substack{t=1\\ l\neq t}}^{3}\Gamma\left(b_t-b_l\right)\Gamma\left(1-a_1+b_t\right)}{\Gamma\left(a_2-b_l\right)\Gamma\left(1-b_4+b_l\right)}$$

3.2. Average Bit Error Rate

The average BER is performed for the binary phase shift keying (BPSK), and the conditional probability of the modulation scheme can be expressed as [14]:

$$P\left(e/\gamma\right) = \frac{1}{2}\, erfc\left(\sqrt{\gamma}\right) \tag{20}$$

The conditional probability of the modulation scheme given in (20) can be expressed in terms of Meijer-G function by using the identity detailed in [14] as:

$$P\left(e/\gamma\right) = \frac{1}{2\sqrt{\pi}}\, G_{1,2}^{2,0}\left(\gamma \,\middle|\, \begin{matrix} 1 \\ 0,\, 1/2 \end{matrix}\right) \tag{21}$$

For easy simplification, the conditional probability of the considered modulation scheme can be represented using McLaurin series expansion as:

$$P\left(e/\gamma\right) = \frac{1}{2}\left[1 - \frac{2}{\pi}\sum_{n=0}^{\infty}\frac{(-1)^n}{n!\,(2n+1)}\,\gamma^{n+1/2}\right] \tag{22}$$

Thus, the average BER for concerned system can be defined as [18]:

$$P_e = P_e\left(\gamma_{RIS}\right) + P_e\left(\gamma_{RD}\right) - P_e\left(\gamma_{RIS}\right) P_e\left(\gamma_{RD}\right) \tag{23}$$

where $P_e(\gamma_{RIS})$ is the average BER of the source-RIS-relay link, and the average BER for the hybrid RF/FSO $P_e(\gamma_{RD})$ can be expressed as:

$$P_e\left(\gamma_{RD}\right) = E_{FSO}\left(\gamma_{th}\right) + P_{out}^{fso}\left(\gamma_{th}\right) E_{RF} \tag{24}$$

where $E_{FSO}(\gamma_{th})$ denotes the average BER of the FSO sub-link when $\gamma_{fso} > \gamma_{th}$; $P_{out}^{fso}(\gamma_{th})$ is the outage probability of the FSO sub-link; E_{RF} signifies the average BER of the RF sub-link. Hence, $E_{FSO}(\gamma_{th})$ can be expressed as:

$$E_{FSO}\left(\gamma_{th}\right) = \underbrace{\int_0^{\infty} P(e/\gamma) f_{FSO}(\gamma) d\gamma}_{A_1} - \underbrace{\int_0^{\gamma_{th}} P(e/\gamma) f_{FSO}(\gamma) d\gamma}_{A_2} \tag{25}$$

By putting (7) and (21) into (25), the A_1 term of (25) can be expressed as:

$$A_1 = \frac{F_{SR}\left(\gamma\right)}{2\sqrt{\pi}} \int_0^{\infty} \gamma^{-1}\, G_{1,2}^{2,0}\left(\gamma \,\middle|\, \begin{matrix} 1 \\ 0,\, 1/2 \end{matrix}\right) G_{1,3}^{3,0}\left(\frac{\Omega\gamma}{\bar{\gamma}_3} \,\middle|\, \begin{matrix} \xi^2+1, \\ \xi^2, \alpha, \beta \end{matrix}\right) d\gamma \tag{26}$$

By utilising the integral identity stated in [36, Eq. (21)], (26) can be solved as:

$$A_1 = \frac{F_{SR}\left(\gamma\right)}{2\sqrt{\pi}}\, G_{3,4}^{3,2}\left(\frac{\Omega}{\bar{\gamma}_3} \,\middle|\, \begin{matrix} \xi^2+1, 1,\, 1/2 \\ \xi^2, \alpha, \beta, 0 \end{matrix}\right) \tag{27}$$

By putting (7) and (22) into (25), the A_2 term of (25) can be expressed as:

$$\begin{aligned} A_2 \;=\; & \frac{\vartheta}{2}\int_0^{\gamma_{th}} \gamma^{-1}\, G_{1,3}^{3,0}\left(\frac{\Omega\gamma}{\bar{\gamma}_3} \,\middle|\, \begin{matrix} \xi^2+1 \\ \xi^2, \alpha, \beta \end{matrix}\right) d\gamma \\ & -\frac{\Psi}{\pi}\sum_{n=0}^{\infty}\frac{(-1)^n}{n!\,(2n+1)}\int_0^{\gamma_{th}} \gamma^{\frac{2n+1}{2}-1}\, G_{1,3}^{3,0}\left(\frac{\Omega\gamma}{\bar{\gamma}_3} \,\middle|\, \begin{matrix} \xi^2+1 \\ \xi^2, \alpha, \beta \end{matrix}\right) d\gamma \end{aligned} \tag{28}$$

By using the integral identity stated in [30, Eq. (2.24.2(2))], (28) can be solved as:

$$\begin{aligned} A_2 \;=\; & \frac{\vartheta}{2}\,\gamma_{th}^{-1}\, G_{2,4}^{3,1}\left(\frac{\Delta\gamma_{th}}{\bar{\gamma}_3} \,\middle|\, \begin{matrix} \xi^2+1,\, 1 \\ \xi^2, \alpha, \beta, 0 \end{matrix}\right) \\ & -\frac{2}{\pi}\sum_{n=0}^{\infty}\frac{(-1)^n}{n!\,(2n+1)}\gamma_{th}^{\frac{2n-1}{2}}\, G_{2,4}^{3,1}\left(\frac{\Omega\gamma_{th}}{\bar{\gamma}_3} \,\middle|\, \begin{matrix} \frac{1}{2}-n,\, \xi^2+1 \\ \xi^2, \alpha, \beta, -\left(n+\frac{1}{2}\right) \end{matrix}\right) \end{aligned} \tag{29}$$

Thus, $E_{FSO}(\gamma_{th})$ can be obtained by invoking (27) and (29) into (24).

Moreover, the outage probability of the FSO sub-link can be obtained as by using (8) as follows:

$$P_{out}^{fso}\left(\gamma_{th}\right) = F_{FSO}\left(\gamma\right) \tag{30}$$

The average BER of the RF sub-link can be expressed as:

$$E_{RF} = \int_{0}^{\infty} P\left(e/\gamma\right) f_{RF}\left(\gamma\right) d\gamma \tag{31}$$

By invoking (5) and (21) into (31), the average BER of the RF sub-link can expressed as:

$$E_{RF} = \frac{1}{2\sqrt{\pi}\,\Gamma\left(m_f\right)\lambda^{m_f}} \int_{0}^{\infty} \gamma^{m_f-1} \exp\left(-\gamma/\lambda\right) G_{1,2}^{2,0}\left(\gamma \,\middle|\, \begin{matrix} 1 \\ 0, 1/2 \end{matrix}\right) d\gamma \tag{32}$$

By applying the integral identity given in [29, Eq. (7.813(1))], (32) can be solved as:

$$E_{RF} = \frac{1}{2\sqrt{\pi}\,\Gamma\left(m_f\right)} G_{2,2}^{2,1}\left(\lambda \,\middle|\, \begin{matrix} 1-m_f,\, 1 \\ 0,\, 1/2 \end{matrix}\right) \tag{33}$$

Hence, $P_e(\gamma_{RD})$ can be determined by putting (25), (30), and (33) into (24).

Also, the average BER of the source-RIS-relay can be defined as:

$$P_e\left(\gamma_{RIS}\right) = \int_{0}^{\infty} P\left(e/\gamma\right) f_{RIS}\left(\gamma\right) d\gamma \tag{34}$$

By substituting (1) and (21) into (34), (34) can be expressed as:

$$P_e\left(\gamma_{RIS}\right) = \varpi \int_{0}^{\infty} \gamma^{\frac{\mu_1-1}{2}} \exp\left(-\gamma^{1/2} \Big/ \sqrt{\bar{\gamma}_1 \mu_2^2}\right) G_{1,2}^{2,0}\left(\gamma \,\middle|\, \begin{matrix} 1 \\ 0,\, 1/2 \end{matrix}\right) d\gamma \tag{35}$$

where $\varpi = \frac{1}{4\sqrt{\pi}\mu_2^{\mu_1+1}\Gamma(\mu_1+1)\bar{\gamma}_1^{(\mu_1+1)/2}}$.

By converting the exponential function to Meijer-G function, (35) can be expressed as:

$$P_e\left(\gamma_{RIS}\right) = \varpi \int_{0}^{\infty} \gamma^{\frac{\mu_1-1}{2}} G_{1,2}^{2,0}\left(\gamma \,\middle|\, \begin{matrix} 1 \\ 0,\, 1/2 \end{matrix}\right) G_{1,2}^{2,0}\left(\frac{\gamma^{\frac{1}{2}}}{\sqrt{\bar{\gamma}_1 \mu_2^2}} \,\middle|\, \begin{matrix} - \\ 0 \end{matrix}\right) d\gamma \tag{36}$$

By utilizing the integral identity detailed in [36, Eq. (21)], (36) can be solved as:

$$P_e\left(\gamma_{RIS}\right) = \varpi G_{2,3}^{2,2}\left(\frac{1}{4\bar{\gamma}_1\mu_2^2} \,\middle|\, \begin{matrix} -\left(\frac{\mu_1-1}{2}\right),\, -\left(\frac{\mu_1-1}{2}\right)-\frac{1}{2} \\ 0,\, \frac{1}{2},\, -\left(\frac{\mu_1-1}{2}\right)-1 \end{matrix}\right) \tag{37}$$

Thus, by substituting (24) and (37) into (23), the exact ABER closed-form expression for the proposed RIS hybrid FSO/RF system is derived.

4. NUMERICAL RESULTS AND DISCUSSIONS

In this section, the numerical results for the performance of reconfigurable intelligent surface in cooperative decode-and-forward relaying for hybrid RF/FSO system is presented under various systems and channel conditions. The validation of the derived expressions through Montel-Carlo simulations is also illustrated. Concerning the influence of atmospheric turbulence, the following turbulence conditions are considered which include: weak levels ($\alpha = 3.78$, $\beta = 3.74$), moderate level ($\alpha = 2.50$, $\beta = 2.06$), and strong levels ($\alpha = 2.04$, $\beta = 1.10$). Except otherwise stated, the system is subjected to strong

turbulence, $N_E = 5$, $\xi = 6.5$, and $m_f = m_i = 2$. Regarding the system without RIS, it is assumed that the source equipped with single antenna communicates directly with the DF relay over Nakagami-m fading channel.

In Figure 2, the impact of number of reflecting elements N_E in RIS on the system performance is presented under different cooperative transmissions. It can be clearly observed that the increase in N_E significantly enhances the system performance for two cooperative transmissions. Therefore, the RIS-Hybrid downlink system outperforms the RIS-FSO downlink system due to switching benefit between the FSO and RF link. In addition, the analytical results perfectly match the simulation results. This observation justifies the accuracy of the derived outage expression.

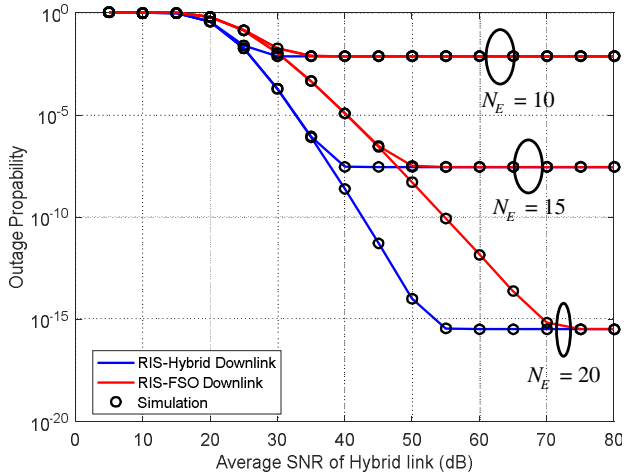

Figure 2. Impact of number of RIS reflecting element on the system performance at $\gamma_{th} = 20\,\text{dB}$, $\bar{\gamma}_1 = 5\,\text{dB}$ and $m_f = m_i = 2$.

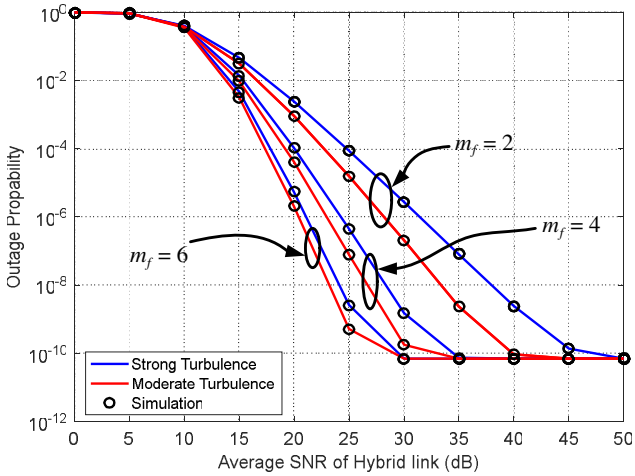

Figure 3. Effect of m_f parameter on the system performance under the different turbulence conditions at $\gamma_{th} = 10\,\text{dB}$ and $\bar{\gamma}_1 = 15\,\text{dB}$.

The effect of fading severity m_f parameter of the RF sub-link under various atmospheric turbulence conditions is demonstrated in Figure 3. It can be inferred from the results that the increase in m_f of the RF sub-link leads to improvement in the quality of link and hence offers the system better performance. However, the results show that the stronger atmospheric turbulence on the FSO sub-link deteriorates the system outage probability performance under the same system conditions.

The influence of pointing errors on the system performance is illustrated in Figure 4 under different cooperative transmissions. The results show that the system performance degrades as the pointing error on FSO sub-link decreases. The lower the value of ξ is, the stronger the impact of pointing error is on the system performance. Also, it can be deduced from the results that the RIS-hybrid downlink system performs better than the RIS-FSO downlink system under the same pointing error conditions. The results also depict that the analytical results perfectly agree with simulation results which justify the accuracy of the derived expression.

The outage performance of the system under different values of threshold SNR γ_{th} for different cooperative transmissions is presented in Figure 5. It can be inferred from the results that the increase in threshold values degrades the system performance with lower value offering the system better performance. Also, the results illustrate that the RIS-hybrid downlink system outperforms the RIS-FSO downlink system. In addition, it can be observed that the asymptotic results are sufficiently tight with the analytical outage values at high SNR which show the correctness of the analytical results.

The system outage performance under the influence of fading severity m_i parameter of the RIS link is illustrated in Figure 6. It can be deduced from the results that the increase in m_i of the link leads to improvement in quality of link and thus offers the system better performance. The results also depict that the use of RIS significantly improves the system outage performance compared to non-RIS system.

In Figure 7, the error rate performance of the system under the influence of fading severity m_i and

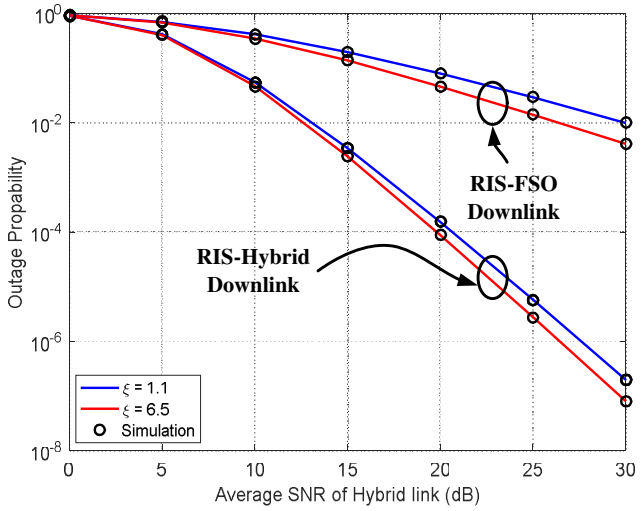

Figure 4. Influence of pointing errors on the system performance at $\gamma_{th} = 5\,\text{dB}$ and $\bar{\gamma}_1 = 15\,\text{dB}$.

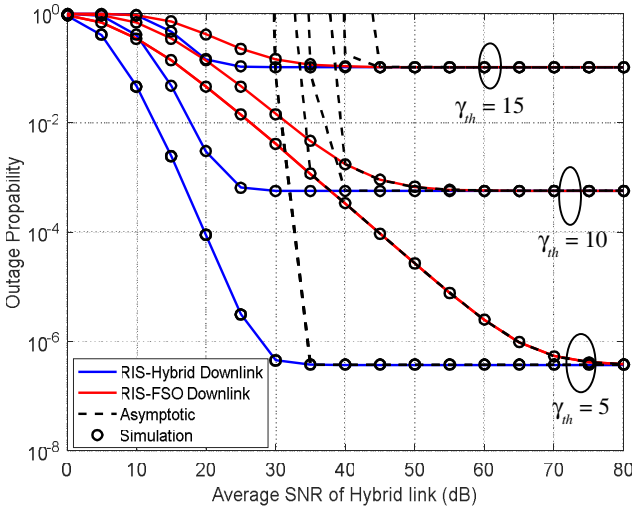

Figure 5. Impact of threshold SNR γ_{th} on the system performance under strong turbulence with $\bar{\gamma}_1 = 5\,\text{dB}$.

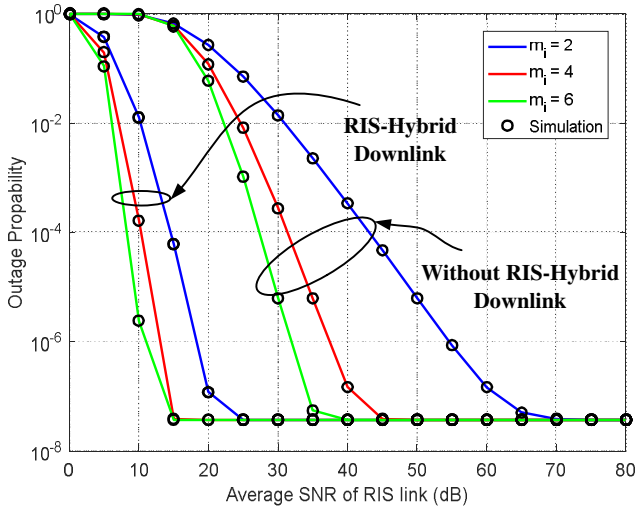

Figure 6. Effect of m_i parameter on the system performance at $\bar{\gamma}_2 = \bar{\gamma}_3 = 5\,\text{dB}$ and $\gamma_{th} = 5\,\text{dB}$.

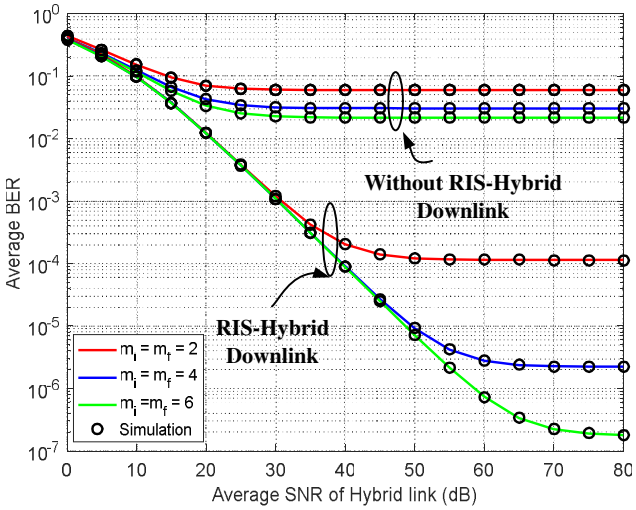

Figure 7. Influence of m_i and m_f parameters on the system error rate $\gamma_{th} = 5\,\text{dB}$ and $\bar{\gamma}_1 = 5\,\text{dB}$.

m_f parameters of the RIS link and RF sub-link receptively are demonstrated. The results show that the increase in fading severity m_i and m_f parameters for the RIS link and RF sub-link significantly enhances the quality of the both links and offers the system better performance. Under the same condition, the system with RIS yields better error rate than the conventional hybrid downlink system without RIS. Moreover, the analytical results corroborate with the simulation results which signifies the accuracy of the derived error rate.

The impact of atmospheric turbulence on the system error rate performance is presented in Figure 8. Similar to Figure 3, the results show that the increase in the atmospheric turbulence from weak to strong level significantly deteriorates the system error rate. Under the same turbulence condition, it can be observed that the RIS-hybrid downlink system yields better performance than the RIS-FSO downlink system due to switching benefit between the FSO and RF links.

The error rate performance of the system under the influence of pointing errors on the FSO sub-link is presented in Figure 9. It can be deduced from the results that the system error rate performance

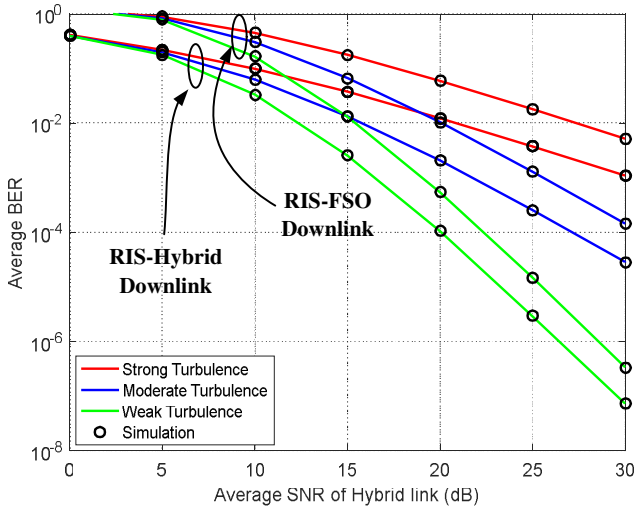

Figure 8. Impact of atmospheric turbulence on the system error rate at, $\gamma_{th} = 5\,\text{dB}$ and $\bar{\gamma}_1 = 15\,\text{dB}$.

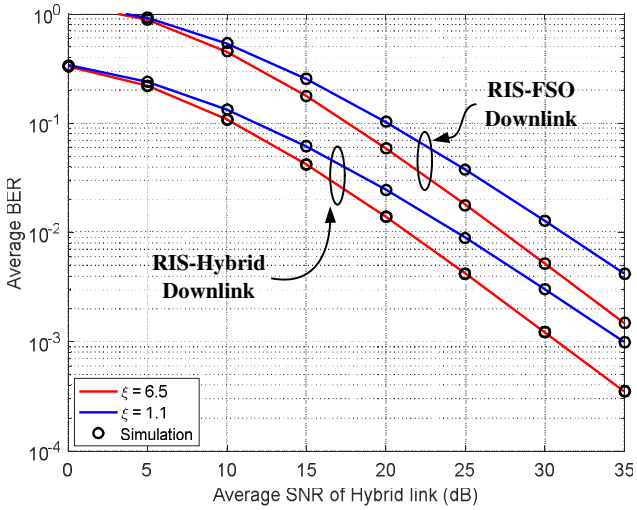

Figure 9. Impact of pointing errors on the system error rate under strong turbulence at $\gamma_{th} = 5\,\text{dB}$ and $\bar{\gamma}_1 = 15\,\text{dB}$.

degrades as the pointing error gets severe. Similar to Figure 4, the lower value of ξ signifies stronger pointing error effect, and the RIS-hybrid downlink system offers better performance than RIS-FSO link. Also, the analytical results match the simulation ones perfectly.

5. CONCLUSION

The performance of RIS in cooperative decode-and-forward relaying for hybrid RF/FSO system is analysed in this study whereby information is transmitted simultaneously on both RF and FSO links of the system downlink. The concerned system closed-form expressions of the outage probability and average BER are obtained. Moreover, the system outage asymptotic expression is derived in order to gain more insight about the analytical outage expression at high SNR. The results show that analytical results perfectly agree with the simulation ones which justify the accuracy of the derived expressions. Also, it is deduced from the results that the asymptotic results tightly match the analytical ones at high SNR. In addition, the results show that the number of reflecting elements in RIS, atmospheric turbulence, pointing error, and Nakagami-m fading severity parameters significantly affect the system performance. Furthermore, it is observed that the hybrid RF/FSO system with RIS outperforms the one without RIS.

REFERENCES

1. Chapala, V. K. and S. Zafaruddin, "RIS-assisted multihop FSO/RF hybrid system for vehicular communications over generalized fading," *arXiv preprint arXiv:.12944*, 2021.
2. Chen, J., Y.-C. Liang, Y. Pei, and H. Guo, "Intelligent reflecting surface: A programmable wireless environment for physical layer security," *IEEE Access*, Vol. 7, 82599–82612, 2019.
3. Basar, E., M. Di Renzo, J. De Rosny, M. Debbah, M.-S. Alouini, and R. Zhang, "Wireless communications through reconfigurable intelligent surfaces," *IEEE Access*, Vol. 7, 116753–116773, 2019.
4. Ibrahim, H., H. Tabassum, and U. T. Nguyen, "Exact coverage analysis of intelligent reflecting surfaces with Nakagami-m channels," *IEEE Transactions on Vehicular Technology*, Vol. 70, No. 1, 1072–1076, 2021.

5. Yang, L., F. Meng, J. Zhang, M. O. Hasna, and M. Di Renzo, "On the performance of RIS-assisted dual-hop UAV communication systems," *IEEE Transactions on Vehicular Technology*, Vol. 69, No. 9, 10385–10390, 2020.
6. Odeyemi, K. O., P. A. Owolawi, and O. O. Olakanmi, "Performance analysis of reconfigurable intelligent surface assisted underwater optical communication system," *Progress In Electromagnetics Research M*, Vol. 98, 101–111, 2020.
7. Mu, X., Y. Liu, L. Guo, J. Lin, and R. Schober, "Simultaneously transmitting and reflecting (STAR) RIS aided wireless communications," *arXiv preprint arXiv:.01421*, 2021.
8. Odeyemi, K. O., P. A. Owolawi, and O. O. Olakanmi, "Reconfigurable intelligent surface-assisted HAPS relaying communication networks for multiusers under AF protocol: A performance analysis," *IEEE Access*, Vol. 10, 14857–14869, 2022.
9. Al-Jarrah, M., A. Al-Dweik, E. Alsusa, Y. Iraqi, and M.-S. Alouini, "On the performance of IRS-Assisted multi-layer uav communications with imperfect phase compensation," *IEEE Transactions on Communications*, Vol. 69, No. 12, 8551–8568, 2021.
10. Odeyemi, K. O., P. A. Owolawi, and O. O. Olakanmi, "On the performance of reconfigurable intelligent surface aided power line communication system under different relay transmission protocols," *Progress In Electromagnetics Research C*, Vol. 111, 119–133, 2021.
11. Odeyemi, K. O. and P. A. Owolawi, "Selection combining hybrid FSO/RF systems over generalized induced-fading channels," *Optics Communications*, Vol. 433, 159–167, 2019.
12. Odeyemi, K. O. and P. A. Owolawi, "Wireless energy harvesting based asymmetric RF/FSO system with transmit antenna selection and receive diversity over M-distribution channel and non-zero boresight pointing error," *Optics Communications*, Vol. 461, 125219, 2020.
13. Shah, S., M. Siddharth, N. Vishwakarma, R. Swaminathan, and A. Madhukumar, "Adaptive-combining-based hybrid FSO/RF satellite communication with and without HAPS," *IEEE Access*, 2021.
14. Sharma, S., A. Madhukumar, and R. Swaminathan, "Switching-based cooperative decode-and-forward relaying for hybrid FSO/RF networks," *Journal of Optical Communications Networking*, Vol. 11, No. 6, 267–281, 2019.
15. Chatzidiamantis, N. D., G. K. Karagiannidis, E. E. Kriezis, and M. Matthaiou, "Diversity combining in hybrid RF/FSO systems with PSK modulation," *2011 IEEE International Conference on Communications (ICC)*, 1–6, IEEE, 2011.
16. Usman, M., H.-C. Yang, and M.-S. Alouini, "Practical switching-based hybrid FSO/RF transmission and its performance analysis," *IEEE Photonics Journal*, Vol. 6, No. 5, 1–13, 2014.
17. Zhang, W., S. Hranilovic, and C. Shi, "Soft-switching hybrid FSO/RF links using short-length raptor codes: Design and implementation," *IEEE Journal on Selected Areas in Communications*, Vol. 27, No. 9, 1698–1708, 2009.
18. Swaminathan, R., S. Sharma, N. Vishwakarma, and A. Madhukumar, "HAPS-based relaying for integrated space-air-ground networks with hybrid FSO/RF communication: A performance analysis," *IEEE Transactions on Aerospace Electronic Systems*, 2021.
19. Yahia, O. B., E. Erdogan, G. K. Kurt, I. Altunbas, and H. Yanikomeroglu, "HAPS selection for hybrid RF/FSO satellite networks," *arXiv preprint arXiv:.12638*, 2021.
20. Ninos, M. P., P. Mukherjee, C. Psomas, and I. Krikidis, "Dual-hop full-duplex DF relay channel with parallel hybrid RF/FSO links," *Proc. IEEE GLOBECOM*, 1–6, 2021.
21. Alathwary, W. A. and E. S. Altubaishi, "On the performance analysis of decode-and-forward multi-hop hybrid FSO/RF systems with hard-switching configuration," *IEEE Photonics Journal*, Vol. 11, No. 6, 1–12, 2019.
22. Tokgoz, S. C., S. Althunibat, S. L. Miller, and K. A. Qaraqe, "Outage analysis of relay-based dual-hop hybrid FSO-mmWave systems," *IEEE Access*, 2021.
23. Verma, G. D., A. Mathur, Y. Ai, and M. Cheffena, "Mixed dual-hop IRS-Assisted FSO-RF communication system with H-ARQ protocols," *IEEE Communications Letters*, 2021.

24. Odeyemi, K. O., G. Aiyetoro, P. A. Owolawi, and O. O. Olakanmi, "Performance analysis of reconfigurable intelligent surface in a dual-hop DF relay empowered asymmetric RF/FSO networks," *Optical Quantum Electronics*, Vol. 53, No. 11, 1–17, 2021.
25. Salhab, A. M. and L. Yang, "Mixed RF/FSO relay networks: RIS-equipped RF source vs RIS-aided RF source," *IEEE Wireless Communications Letters*, Vol. 10, No. 8, 1712–1716, 2021.
26. Sikri, A., A. Mathur, P. Saxena, M. R. Bhatnagar, and G. Kaddoum, "Reconfigurable intelligent surface for mixed FSO-RF systems with co-channel interference," *IEEE Communications Letters*, Vol. 25, No. 5, 1605–1609, 2021.
27. Malik, S., P. Saxena, and Y. H. Chung, "Performance analysis of a UAV-based IRS-assisted hybrid RF/FSO link with pointing and phase shift errors," *Journal of Optical Communications Networking*, Vol. 14, No. 4, 303–315, 2022.
28. Samuh, M. H. and A. M. Salhab, "Performance analysis of reconfigurable intelligent surfaces over Nakagami-m fading channels," *arXiv preprint arXiv:.07841*, 2020.
29. Gradshteyn, I., I. Ryzhik, and R. H. Romer, *Tables of Integrals, Series, and Products*, 7th Ediiton, Academic Press, 1988.
30. Prudnikov, A., Y. A. Brychkov, and O. Marichev, *Integrals and Series. Volume 3: More Special Functions*, Taylor and Francis, Oxford, UK, 2003.
31. Nguyen, N.-T., H.-N. Nguyen, N.-L. Nguyen, A.-T. Le, D.-T. Do, and M. Voznak, "Enhancing spectrum efficiency for multiple users in hybrid satellite-terrestrial networks," *IEEE Access*, Vol. 9, 50291–50300, 2021.
32. Ndjiongue, A. R., T. Ngatched, O. A. Dobre, A. G. Armada, and H. Haas, "Performance analysis of RIS-based nT-FSO link over GG turbulence with pointing errors," *arXiv preprint arXiv:.03654*, 2021.
33. Odeyemi, K. O., P. A. Owolawi, and V. M. Srivastava, "Performance analysis of free space optical system with spatial modulation and diversity combiners over the Gamma Gamma atmospheric turbulence," *Optics Communications*, Vol. 382, 205–211, 2017.
34. Lei, H., Y. Zhang, K.-H. Park, I. S. Ansari, G. Pan, and M.-S. Alouini, "Performance analysis of dual-hop RF-UWOC systems," *IEEE Photonics Journal*, Vol. 12, No. 2, 1–15, 2020.
35. Li, S., L. Yang, D. B. Da Costa, and S. Yu, "Performance analysis of UAV-based mixed RF-UWOC transmission systems," *IEEE Transactions on Communications*, 2021.
36. Adamchik, V. and O. Marichev, "The algorithm for calculating integrals of hypergeometric type functions and its realization in REDUCE system," *Proceedings of the International Symposium on Symbolic and Algebraic Computation*, 212–224, 1990.